Scientific Research Publishing

Open Journal of Applied Sciences, 2024, 14, 589-608
https://www.scirp.org/journal/ojapps
ISSN Online: 2165-3925
ISSN Print: 2165-3917

Experimental Investigation of the Stability of the Performance Characteristics of a Photovoltaic Module in the Face of Environmental and Meteorological Factors

Adingra Paul Arsène Kouassi*, Siaka Touré, Diakaridja Traoré

Laboratoire des Sciences de la Matière, de l'Environnement et de l'Energie Solaire (LASMES), Unité de Formation et de Recherche des Sciences des Structures de la Matière et Technologie (UFR-SSMT), Université Félix Houphouët Boigny, Abidjan, Côte d'Ivoire
Email: *debouegla@yahoo.fr

How to cite this paper: Kouassi, A.P.A., Touré, S. and Traoré, D. (2024) Experimental Investigation of the Stability of the Performance Characteristics of a Photovoltaic Module in the Face of Environmental and Meteorological Factors. *Open Journal of Applied Sciences*, **14**, 589-608.
https://doi.org/10.4236/ojapps.2024.142042

Received: January 4, 2024
Accepted: February 26, 2024
Published: February 29, 2024

Abstract

The explosive technological improvement of photovoltaic systems as well as the necessity of populations to come to less expensive energy sources, that have led to an implosion at the level of solar panel manufacturers. This causes a large flow of these equipments to developing countries where the need is high, without any quality control. That conducted an experimental investigation on the performance characteristics of a 250 wp monocrystalline silicon photovoltaic module in other to check the verification and quality control. Most of these PV panels which often have missing informations are manufactured and tested in places that are inadequate for our environmental and meteorological conditions. Also, their influences on the stability of internal parameters were evaluated in order to optimize their performance. The results obtained at maximum illumination (1000 w/m^2) confirmed those produced by the manufacturer. The analysis of these characteristics showed that the illumination and the temperature (meteorological factors) influenced at most the stability of the internal characteristics of the module in the sense that the maximum power increased very rapidly beyond 750 w/m^2 but a degradation of performance was accentuated for a temperature of the solar cells exceeding 50˚C. The degradation coefficients were evaluated at −0.0864 V/˚C for the voltage and at −1.6248 w/˚C for the power. The 10˚ inclination angle of the solar panel proved to be ideal for optimizing overall efficiency in practical situations.

Keywords

Renewables Energies Instruments, Internal Parameters of Photovoltaic Panel, Monocrystalline Photovoltaic Panel, Solar Energy Production, Energy

Intermittence

1. Introduction

Solar energy is an important source of renewable energy that is an alternative to the depletion of fossil energy sources [1] [2] and inaccessibility to fissile energy in developing countries [3]. The relentless pursuit of sustainable energy solutions has propelled photovoltaic (PV) technology into the forefront of renewable energy sources [3] [4] [5]. As the demand for solar power continues to escalate, it becomes imperative to scrutinize the stability of performance characteristics exhibited by PV modules, especially in the dynamic context of varying environmental and meteorological conditions [6] [7].

Suitable for small and medium power applications, this energy is a development engine for remote and isolated areas of conventional power distribution lines. The photovoltaic module that is the centerpiece of this technology, deserves a careful study of its parameters before its use since these fluctuate constantly with certain external factors [8]. For a photovoltaic installation, the change of 50% in illumination automatically causes a degradation of 50% in the power supplied by the photovoltaic generator [9].

The instability and vulnerability of silicon-based solar cells to environmental and meteorological factors has led to a considerable increase in research efforts aimed at developing solar cells based on organic and hybrid materials [10] [11] [12]. These technologies have shown great performance, gradually gaining ground in the architecture markets [8].

Various methods have also been found to effectively prevent potential induced degradation (PID) in P-type C-Si modules [13], as they dominate the present PV market. The PID progression in standard C-Si modules depends on applied voltage, humidity and temperature. The leakage current exhibits an Arrhenius-type relationship with temperature. Humidity and applied voltage also affect the PID in many ways.

The exploration of photovoltaic (PV) materials reflects the ongoing search for sustainable energy solutions. An analysis has been made of the significant advances made in this field, from the refinement of silicon-based solar cells, the development of thin-film technologies and the emergence of materials such as perovskites [14]. Every advance brings us closer to a future where sustainable energy is not just a goal, but a reality. Silicon-based cells have long been the backbone of the solar industry. Thin-film technologies have emerged as a compelling alternative, offering versatility and cost-effectiveness with a smaller material footprint. Renewed interest in perovskite solar cells has reshaped the research landscape, with their potential for high efficiency and low-cost production attracting keen interest worldwide.

This experimental investigation aims to shed light on the intricate interplay

between the performance of a photovoltaic module and the myriad factors in its external surroundings.

Our study deals with the experimental evaluation of the characteristics of the monocristalline photovoltaic module of 250 wp in order to analyze their stability against meteorological and environmental factors of the implantation site. For this, the electrical and performance characteristics of the photovoltaic module were determined, and the effect of the variation of the instantaneous illumination, cell temperature and tilt angle on the stability of the internal characteristics of the PV module was assessed directly at the installation site.

In this context, our study seeks to expand upon the existing body of knowledge by providing a nuanced investigation into the stability of specific performance characteristics of a photovoltaic module. Through a series of controlled experiments and meticulous data analysis, we aim to contribute actionable insights that can inform the design, maintenance, and optimization of solar energy systems in the face of dynamic environmental and meteorological influences.

2. Materials and Methods

2.1. Methodology

The experiments were carried out on the roof of a building 10 m above ground level at the Félix Houphouët-Boigny University in Abidjan. The longitude and latitude of the site are respectively 5˚18'34"North and 4˚00'45"West. For different values of the overall illumination measured by a thermoelectric pyranometer, the short circuit current (I_{sc}), the open circuit voltage (V_{oc}) and the ambient temperature (T_a) were determined. Using a platinum resistance probe connected to the photovoltaic module, the cells temperature was evaluated. The current-voltage characteristics (I-V) were also obtained according to the atmospheric conditions of the site and the tilt angles of the solar collector of 5˚, 10˚ and 15˚, oriented towards the south with respect to the horizontal.

2.2. Annual Variation of Sunshine in Abidjan

The sunshine data for the city of Abidjan from 1978 to 1988 [15] and from 2003 to 2009 [16] show that the average daily sunshine duration is 6.5 hours. The average daily irradiation values from 1978 to 1988 and from 2003 to 2009 are respectively 4446 wh/m^2.d and 3875 wh/m^2.d. During these years the sunniest months are the months of February, March and April. The maximum value of the overall irradiation is of the order of 5184 wh/m^2.d in April. The least sunny months are June, July and August. These months correspond to the rainy seasons in Abidjan.

The sunshine measurements made at the site in 2017 resulted in an average annual global irradiation value of 3331 wh/m^2.d. In this year, a maximum value of solar irradiation recorded of 4403 wh/m^2.d in April and a minimum value of 2351 wh/m^2.d in the month of June. The annual variations in global irradiation

are shown in Figure 1. They show a variability of available solar energy from 1978 to 1988, then from 2003 to 2009 and in 2017 [17]. However, the annual distribution of solar energy potential in Abidjan typically retains the same type of variation when moving from one year to another.

On-site illumination measurements yielded maximum values in the order of 1009 w/m^2 in March. The performance of a photovoltaic panel is related to meteorological parameters. It is therefore important to check its compatibility with the climatic conditions of the installation site.

2.3. Some Characteristic Parameters of the Photovoltaic Module

The essential electrical characteristics of a photovoltaic panel are the short circuit current (I_{sc}), the open circuit voltage (V_{oc}) and the maximum power (P_m). These parameters that characterize the PV module are a function of the incident illumination (E) and the temperature of the photovoltaic cells (T_c). The values of I_{sc} are slightly influenced by temperature. On the other hand, those of V_{oc} and P_m decay rapidly when the cells temperature increases [18]. A platinum resistance probe in direct contact with the back surface of the cell is used to assess the cell temperature. This technique makes it possible to approximately determine the actual temperature of the photovoltaic cells on the module [18]. The relationship between the probe resistance R_c (Ω) and the cell temperature T_c (˚C) is given by the relation (1).

$$T_c = 2.2611R_c - 223.71 \quad (1)$$

The intensity I(A) of the current supplied by a real photocell under illumination is [19]:

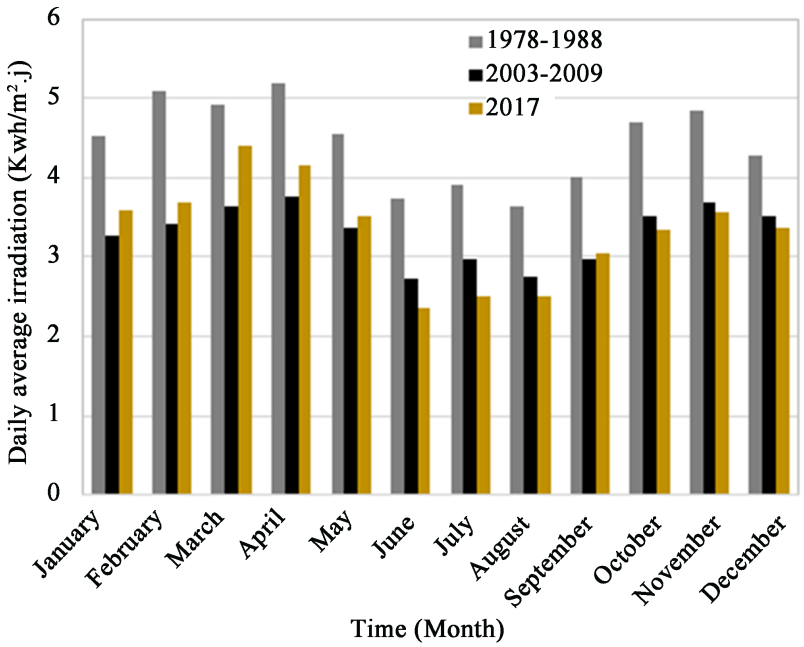

Figure 1. Daily average irradiation of Abidjan city from 1978 to 1988, from 2003 to 2009 and in 2017.

$$I = I_{ph} - I_s\left[\exp\left(\frac{qV + R_s I}{nKT}\right) - 1\right] - \frac{V + R_s I}{R_{sh}} \quad (2)$$

where I_{ph} is the photocurrent, I_s the saturation current of the diode, n ideality factor of the diode, K Boltzmann constant (1.38×10^{-23} J/K), q elementary load (1.602×10^{-19} C), T cell temperature (K), R_s series resistance (Ω) and R_{sh} shunt resistance (Ω).

The short-circuit current (I_{sc}) is obtained for $V = 0$. I_{sc} was measured by connecting an ammeter directly to the PV module terminals.

The open circuit voltage V_{oc} is obtained for $I = 0$ ($I_{ph} = I_{sc}$):

$$V_{oc} = \frac{nKT}{q}\ln\left(\frac{I_{sc}}{I_s}\right) \quad (3)$$

The value of V_{oc} is measured by directly connecting a voltmeter to the PV module terminals.

A photovoltaic module is also characterized by its series resistance R_s and shunt resistance R_{sh}. R_s is due to the resistivity of the material used for the fabrication of the photocells, to the contact resistances and the collector grid. This series resistance, which characterizes all current losses due to contact at the junction, reduces the value of the short-circuit current when it has a high value [20]. As for the shunt resistance R_{sh}, it reports leakage currents in the module. When the value of R_{sh} is low, this leads a large decrease in the open circuit voltage V_{oc} [21]. In this case, the value of the voltage at the PV module terminals becomes very low for the small illuminations.

Various methods have been developed for the determination of R_s and R_{sh} [22] [23] [24]. In our study, The graphical method [25] is used for the evaluation of the series resistance R_s. In practice, the method consists in choosing two I-V curves at different illuminations but at the same temperature. The arbitrary choice of these two characteristics I-V is such that ΔI, which is the variation between the short circuit current I_{sc} and maximum useful current I_m, is the same for both characteristics (**Figure 2**).

From Equation (2), neglecting the term $\frac{V + R_s I}{R_{sh}}$ ($R_{sh} \gg R_s$), at the point of

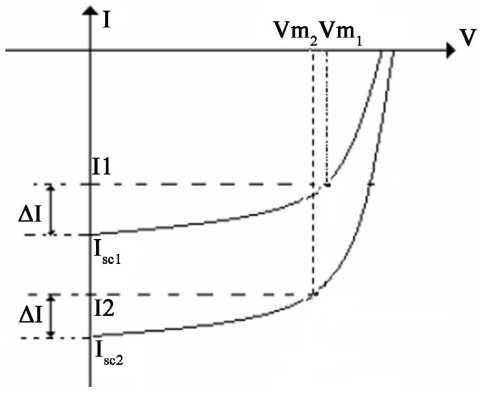

Figure 2. Graphic method of determination of the series resistance

short-circuit ($I_{ph} = I_{sc}$),

The expressions obtained according to the two illuminations are:

$$I_1 = I_{sc1} - I_s\left[\exp\left(\frac{q\left(V_1 + R_s I_1\right)}{nKT}\right) - 1\right] \tag{4}$$

$$I_2 = I_{sc2} - I_s\left[\exp\left(\frac{q\left(V_2 + R_s I_2\right)}{nKT}\right) - 1\right] \tag{5}$$

ΔI defines as follows:

$$\Delta I = I_{sc1} - I_1 = I_{sc2} - I_2 \tag{6}$$

and the following equations obtained:

$$\exp\left(\frac{q\left(V_1 + R_s I_1\right)}{nKT}\right) = \exp\left(\frac{q\left(V_2 + R_s I_2\right)}{nKT}\right) \tag{7}$$

$$V_1 + R_s I_1 = V_2 + R_s I_2 \tag{8}$$

$$R_s = \frac{V_2 - V_1}{I_1 - I_2} \tag{9}$$

Since

$$I_1 - I_2 = I_{sc1} - I_{sc2} \tag{10}$$

and by identifying the voltages V_1 and V_2 at the point of maximum power, the expression of series resistance R_s is determined by:

$$R_s = \frac{V_{m2} - V_{m1}}{I_{sc1} - I_{sc2}} \tag{11}$$

The shunt resistance R_{sh} is also determined from an experimental method which consists to evaluate the slope of the I-V characteristic at the point of short-circuit ($I = I_{sc}$) [26] according to **Figure 3**.

In the region of the curve I-V where the cell behaves like a constant current

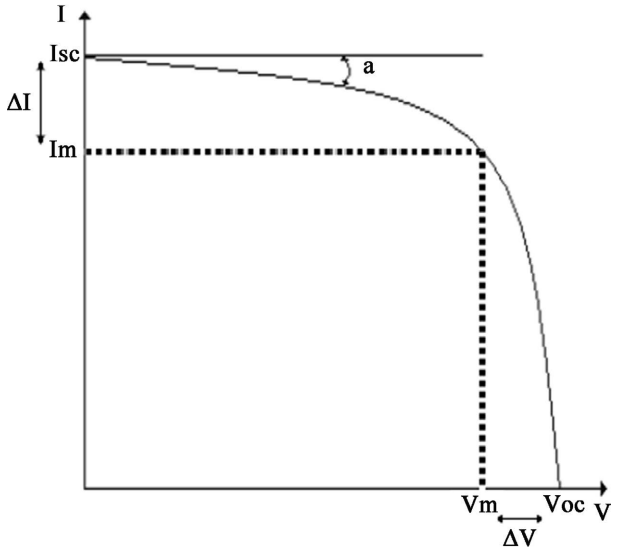

Figure 3. Graphic method of determination of the shunt resistance.

generator ($V = 0$), the Equation (2) is written:

$$I = I_{ph} - \frac{V + IR_s}{R_{sh}} \tag{12}$$

Differentiating the relation (2) at the point of short-circuit ($I_{ph} = I_{sc}$), the following expression is:

$$\frac{\mathrm{d}I}{\mathrm{d}V} | I_{sc} = -\frac{1}{R_{sh}} \tag{13}$$

According to Figure 3, the expression of the shunt resistance is defined by the relation (14).

$$R_{sh} = -\frac{\Delta V}{\Delta I} = \frac{V_m}{I_{sc} - I_m} \tag{14}$$

Figure 4 presents the equivalent diagram of a real photopile to one diode.

Other internal characteristics of the module such as the nominal operating cell temperature (NOCT) and the diode ideality factor (n) can be evaluated from certain experimental linear correlations.

2.4. Current-Voltage Characteristic

The current-voltage characteristic I-V of the module is obtained by varying a resistive load connec-ted to the PV module terminals. The block diagram is shown in Figure 5 and the experimental device in Figure 6.

For tilt angles of 5˚, 10˚ then 15˚ and for different illuminations, the values of the current I and the voltage V at the PV module terminals are noted. The values

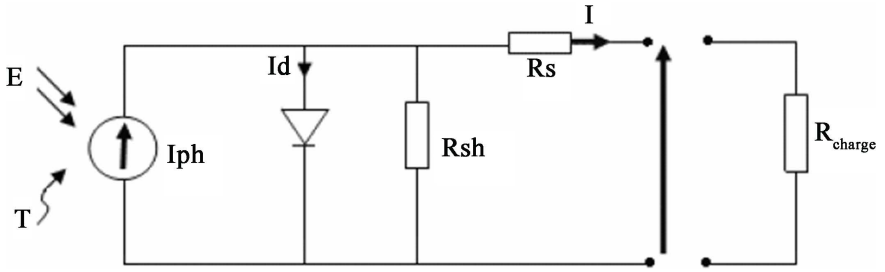

Figure 4. Diagram of a real photopile to one diode.

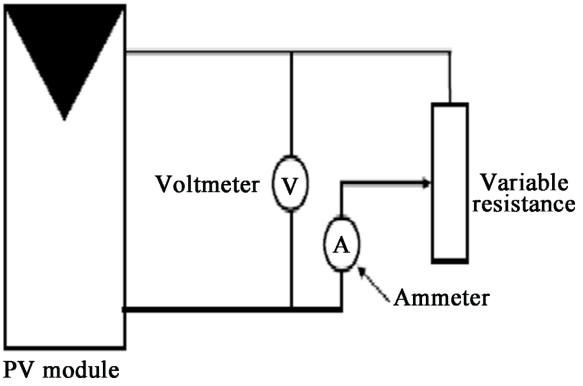

Figure 5. Wiring diagram to note the I-V characteristic.

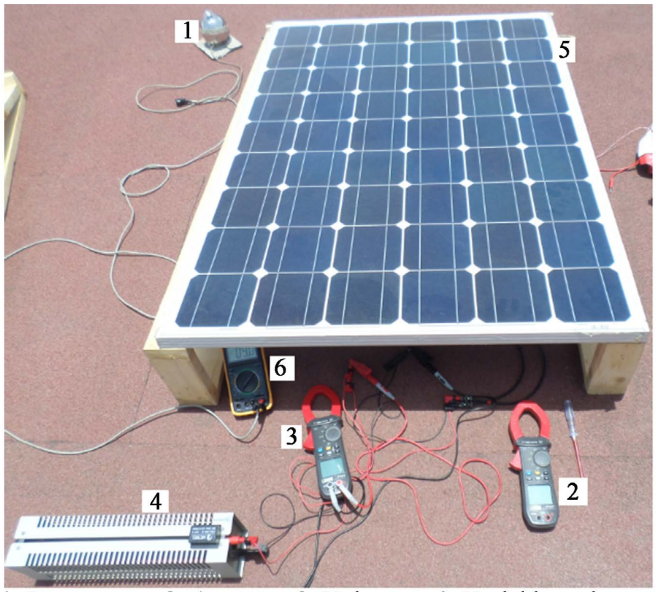

1. Paranometer 2. Ammeter 3. Voltmeter 4. Variable resistance
5. PV module 6. Ohmmeter

Figure 6. Characterization device.

of I and V noted allow the determination of the electrical power P supplied by the module according to relation (5).

$$P = I \cdot V \tag{15}$$

If I_m and V_m are the respective values of I and V for which the electric power is maximal, the maximal power is:

$$P_m = I_m \cdot V_m \tag{16}$$

The couple (I_m; V_m) is determined from the P-V characteristic whose peak represents the maximum power point (V_m; P_m).

3. Results and Discussions

3.1. Electrical Characteristics of the PV Panel at Maximum Illumination on the Site

The different tests carried out allowed us to obtain the current-voltage I-V and power-voltage P-V characteristics of the photovoltaic module for a maximum illumination of 1009 w/m^2. The curves of variation obtained for the tilts 5˚, 10˚ and 15˚ are presented in **Figure 7**.

The analysis of the curves of **Figure 7** makes it possible to deduce the values of I_{sc}, V_{oc}, I_m, V_m and P_m at the maximum illumination under the conditions of the site. The different values are summarized in **Table 1**.

For the photovoltaic module used, the values obtained are most often different from those provided when the module operates under Standard Test Condition (STC).

The current I_{sc} values determined experimentally are slightly higher than those given by the manufacturer. This rise is mainly due to the increase of the solar cell temperature during the experiment. At the point of maximum power,

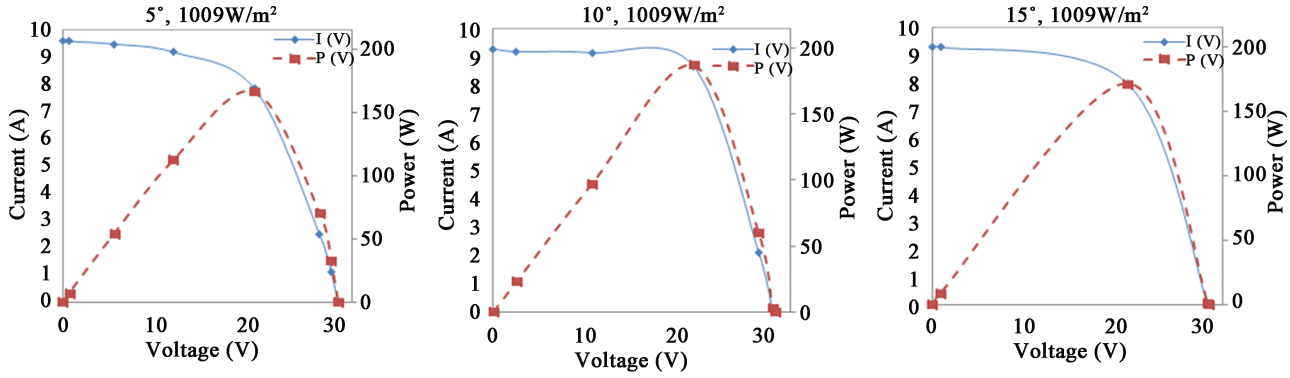

Figure 7. I-V and P-V characteristics at maximum illumination of 1009 w/m² for the tilts 5˚, 10˚ and 15˚.

Table 1. Verification of the electrical characteristics of the PV module.

Parameters tilt angle	manufacturer's data	Experimental values		
		5˚	10˚	15˚
I_{scmax} (A)	9.2	9.6	9.3	9.3
V_{ocmax} (V)	42	30.5	30.4	30.4
I_m (A)	8	8	8.8	8
V_m (V)	36	22.2	21.6	21.5
P_m (w)	288	177.6	190.1	172
E (w/m²)	1000	1009	1009	1009
T_c (˚C)	25	57	54	51

lower values of V_m and P_m are obtained. Those of the maximum intensity I_m are not very different from the value obtained in the Standard Test Condition.

3.2. Influence of Illumination and Temperature on the Electrical Characteristics of the PV Module

For each value of the tilt angles of the PV module, I-V and P-V characteristics at constant temperature as a function of the illumination (Figure 8) then at constant illumination as a function of temperature (Figure 9) have been determined.

At constant temperature, the value of the current increases with illumination. Likewise, the values of the parameters I_{sc}, V_{oc} and P_m increase with illumination. The point of maximum power evolves vertically with the increase of the illumination. This variation of P_m, which is practically constant voltage, is more related to that of the intensity of the current (Table 2), hence the name of the photovoltaic generator of "current generator".

Figure 9 shows that at constant illumination, the maximum power P_m decreases with increasing temperature. Table 2 shows the values of current, voltage and power at the point of maximum power at constant temperature for different angles (5˚, 10˚ and 15˚)

Figure 10 shows the evolution of the maximum power as a function of the

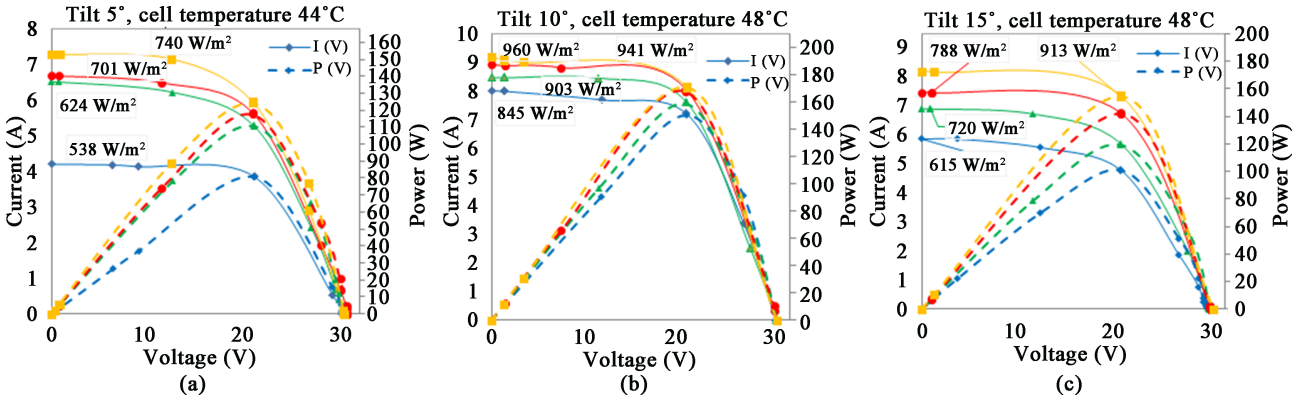

Figure 8. Influence of illumination on the I-V and P-V characteristic.

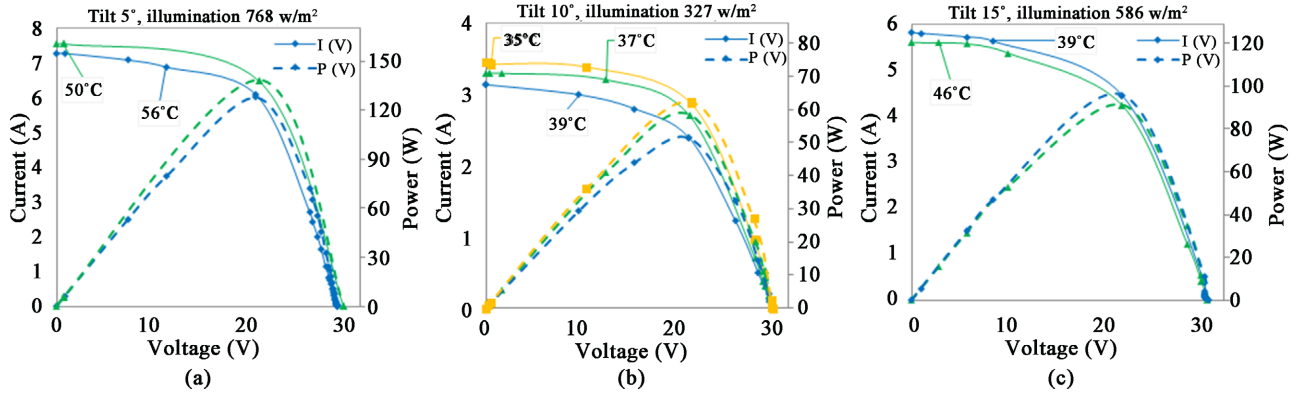

Figure 9. Influence of temperature on the I-V and P-V characteristic.

Table 2. Values of the maximum power according to the illumination and tilt angle of the PV module.

Tilt angle of the PV module	Cell temperature (°C)	Illumination (w/m²)	V_m (V)	I_m (A)	P_m (w)
	44	538	21.1	3.9	82.3
5°	44	624	21.6	4.3	92.9
	44	701	21.5	5.4	116.1
	44	740	21.3	6	127.8
	48	845	21.1	7.2	151.9
10°	48	903	21.4	7.4	158.4
	48	941	21.6	8	172.8
	48	960	21.7	8.2	177.9
	48	615	21	4.8	100.8
15°	48	720	21.7	5.7	123.7
	48	788	21.2	6.8	144.2
	48	913	21.4	7.4	158.4

illumination (Figure 10(a)) and the cell temperature (Figure 10(b)).

The maximum power increases with illumination and temperature between 20 and 200 w. At maximum illumination (1000 w/m²), the experimental value determined maximum power (190 w, 55˚C) is less than the value given by the module manufacturer (250 w; 25˚C). This difference is explained by the fact that the rise in the cell temperature automatically causes a drop in power, with a degradation coefficient of about −1.62 w/˚C. Some works provide a decrease of 4% for an illumination of 1000 w/m² [6]. It is noted that the electrical power supplied by the PV module is proportional to the illumination. It is the tilt angle of 10˚ which makes it possible to obtain values slightly higher compared to inclinations 5˚ and 15˚. In Figure 10(b), an increase in the cell temperature causes a drop in the maximum power above 47˚C.

The effect of the variation of the illumination on the values of the short-circuit current I_{sc} and of the open circuit voltage V_{oc} is observed through the graphs of Figure 11 for different tilt angles of the PV module.

The short-circuit current Isc increases linearly with illumination. However, the value of the open circuit voltage V_{oc} increases slightly for low illuminances

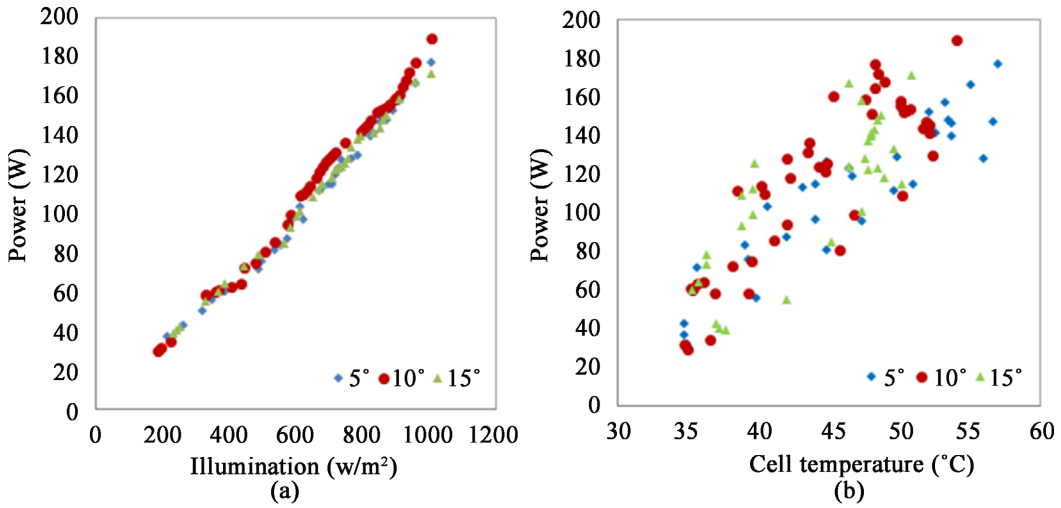

Figure 10. Maximum power according to the illumination and the temperature.

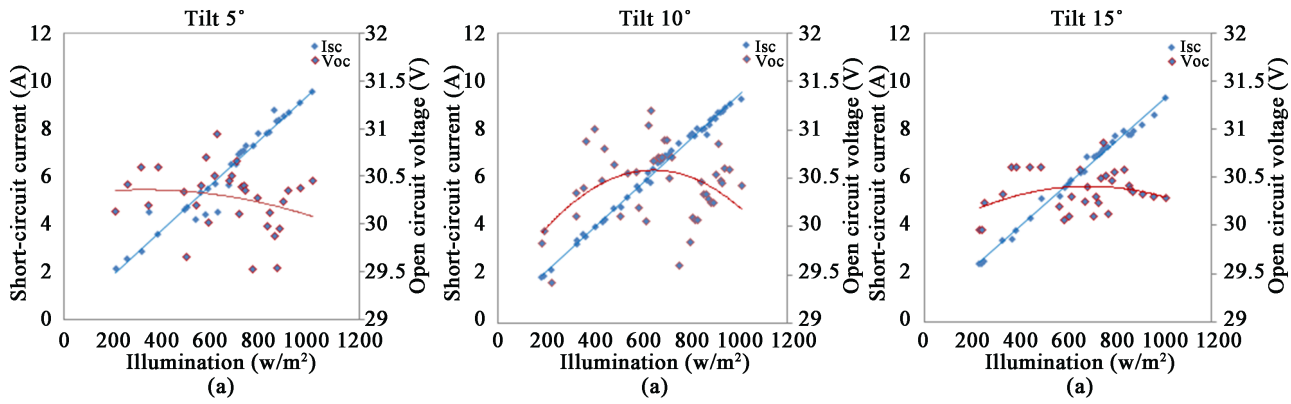

Figure 11. Variation of current I_{sc} and voltage V_{oc} as a function of illumination.

(<600 w/m²) and falls below this value. This reduction of V_{oc} for the strong illuminations is due to the heating of the photovoltaic cells. According to these I-V and P-V characteristics, an increase in temperature considerably reduces the electrical productivity of the photovoltaic panel.

3.3. Evaluation of the Internal Characteristics of the Photovoltaic Module

Certain characteristic parameters such as the series resistance (R_s), the shunt resistance (R_{sh}) and the nominal operating cell temperature (NOCT) are not most often written on the photovoltaic module. The evaluation of these parameters helps to judge the reliability of the module in the meteorological conditions of the experimental site.

However, the constant variation of the resistances R_s and R_{sh} makes their determination very often difficult. For this study, therelations (11) and (14) are used respectively to evaluate them. The results are summarized in Tables 3-5

Table 3. Values of the series and shunt resistances for a tilt of 5˚.

T_c (˚C)	E_1 (w/m²)	E_2 (w/m²)	I_{sc1} (A)	I_{sc2} (A)	I_{m1} (A)	I_{m2} (A)	V_{m1} (V)	V_{m2} (V)	R_s (Ω)	R_{sh1} (Ω)	R_{sh2} (Ω)
35	259	317	2.6	2.9	2.0	2.4	21.5	21.4	0.333	35.8	43.0
39	500	557	4.7	5.3	3.5	3.9	21.7	21.5	0.333	18.1	15.4
44	538	740	4.2	7.3	3.9	6.0	21.1	21.3	0.100	70.3	16.4
44	624	701	4.5	6.5	4.3	5.4	22.5	21.5	0.500	112.5	19.6
54	826	913	7.8	8.7	6.4	7.3	21.8	21.5	0.333	15.6	15.4
54	855	874	8.4	8.8	6.8	6.8	21.6	21.7	0.250	10.8	13.6
57	865	1009	8.3	9.6	6.8	8.0	21.6	22.2	0.461	14.4	13.9

Table 4. Values of the series and shunt resistances for a tilt of 10˚.

T_c (˚C)	E_1 (w/m²)	E_2 (w/m²)	I_{sc1} (A)	I_{sc2} (A)	I_{m1} (A)	I_{m2} (A)	V_{m1} (V)	V_{m2} (V)	R_s (Ω)	R_{sh1} (Ω)	R_{sh2} (Ω)
35	365	403	3.6	4.0	2.8	2.9	21.5	21.4	0.250	26.9	19.5
37	221	432	2.2	4.2	1.6	3.0	21.2	21.5	0.150	35.3	17.9
42	538	576	5.2	5.7	4.0	4.4	21.5	21.6	0.200	17.9	16.5
45	672	692	6.7	6.9	5.6	5.9	21.6	21.5	0.500	19.6	21.5
48	845	922	8.0	8.7	7.2	7.7	21.1	21.4	0.429	26.4	21.4
48	941	961	8.9	9.1	8.0	8.2	21.6	21.7	0.500	24.0	24.1
50	615	855	5.9	8.0	5.1	7.1	21.3	21.5	0.100	26.6	23.9
50	865	874	7.8	8.2	7.1	7.2	21.5	21.4	0.250	30.7	21.4
50	884	895	8.4	8.5	7.3	7.3	21.5	21.6	0.500	19.6	18.0
52	711	817	7.0	7.8	6.0	6.8	21.7	21.4	0.375	21.7	21.4

Table 5. Values of the series and shunt resistances for a tilt of 15˚.

T_c (˚C)	E_1 (w/m²)	E_2 (w/m²)	I_{sc1} (A)	I_{sc2} (A)	I_{m1} (A)	I_{m2} (A)	V_{m1} (V)	V_{m2} (V)	R_s (Ω)	R_{sh1} (Ω)	R_{sh2} (Ω)
37	250	442	2.5	4.3	2.0	3.5	21.4	20.8	0.333	42.8	26.0
40	605	749	5.7	7.2	4.8	6.0	20.8	21.1	0.200	23.1	17.6
47	615	720	5.9	6.9	4.8	5.7	20.9	21.4	0.500	19.0	17.8
47	759	913	7.3	8.2	6	7.4	21.5	21.4	0.111	16.5	26.8
48	711	730	6.9	7.0	5.6	5.9	21.0	20.8	0.200	16.2	18.9
48	797	855	7.7	7.8	6.6	6.7	21.1	21.3	0.111	17.6	19.4
48	865	874	7.8	7.9	6.9	7.1	21.4	21.3	0.444	23.8	26.6
50	682	768	6.8	7.3	5.3	6.2	21.5	21.6	0.200	14.3	19.6

respectively for the inclinations 5˚, 10˚ and 15˚.

For the 5˚ position of the solar collector, there is a strong variation of the series resistance R_s with the illumination E and the cells temperature T_c, a variation rate of 87% ($0.1\Omega < R_s < 0.5\Omega$). Also, the same effects have been noticed on the shunt resistance R_{sh} side with a rate of change in the range of 90% ($10.8\Omega < R_{sh} < 112.5\Omega$).

The 10˚ configuration shows values of the series resistance R_s between 0.1 and 0.5 Ω depending on the variation of the illumination and the cells temperature, a variation rate 87%. As for the shunt resistance R_{sh}, a variation recorded in the rate of 53% ($16.5\Omega < R_{sh} < 35.3\Omega$).

For a tilt of 15˚, a variation of the resistances R_s and R_{sh} is observed respectively of the order of 87% and 67% with the illumination and the temperature.

From a general point of view, variations in illumination and temperature strongly influence the values of the series and shunt resistances. This variation of R_s is between 0.1Ω and 0.5Ω and remains the same whatever the tilt angle of the solar panel is. The variation rate of R_{sh} decreases with increasing of the tilt angle of the module (from 90% to 67%). The variations of these parameters which characterize the losses of contact and leakage of the cells, are represented as a function of the illumination in **Figure 12** and of the temperature in **Figure 13** for each of the tilt angle 5˚, 10˚ and 15˚. Despite of the constance of the variation of these parameters over time we note globally that the series resistance increases with the illumination and the cells temperature while the shunt resistance decreases. Then, if the value of R_s is high (or R_{sh} is small), the higher the current losses in the cells, is, the less productive the photovoltaic module we get.

The cell temperature is defined by the relation (17) [27].

$$T_c = T_a + \frac{E}{800}(\text{NOCT} - 20) \tag{17}$$

Then:

$$T_c - T_a = \frac{E}{800}(\text{NOCT} - 20) \tag{18}$$

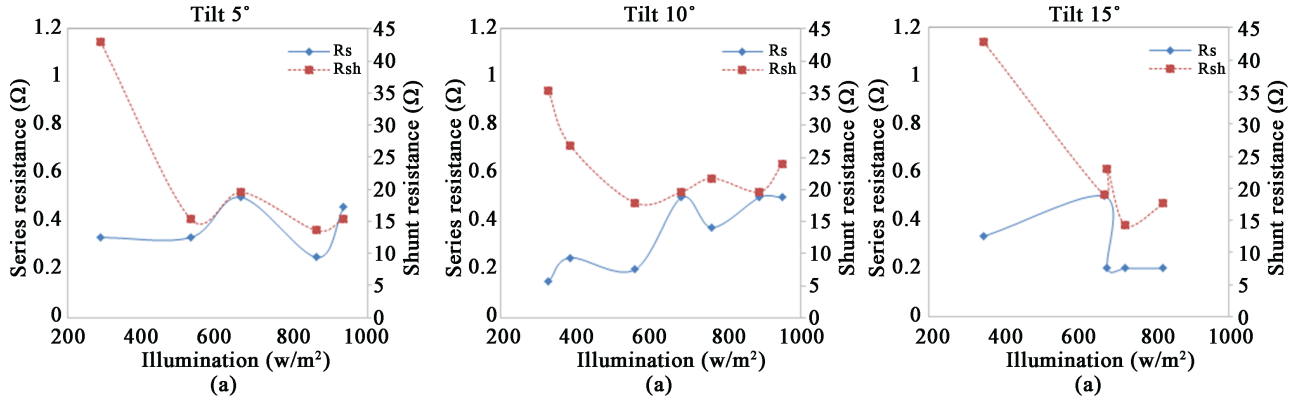

Figure 12. Evolutions of the series and shunt resistances according to the illumination.

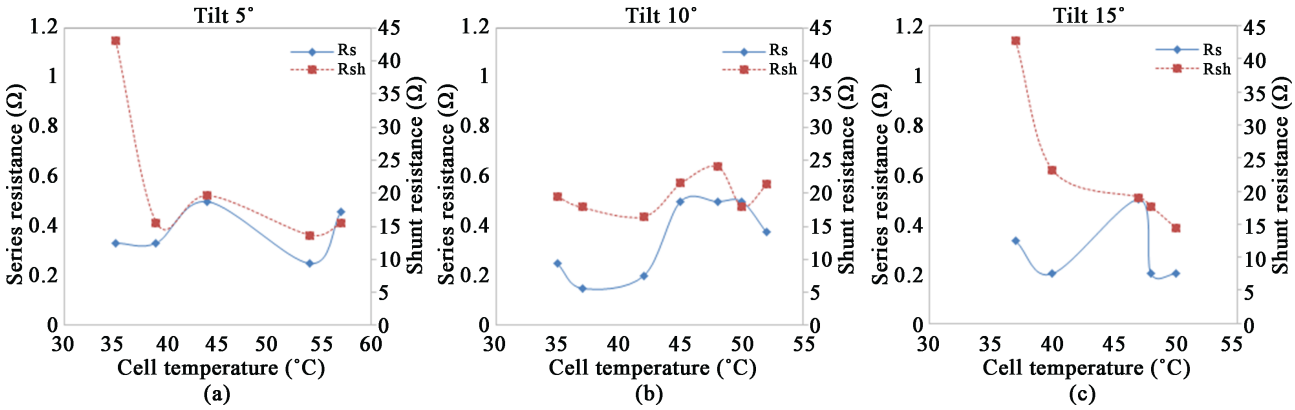

Figure 13. Evolutions of the series and shunt resistances according to the temperature.

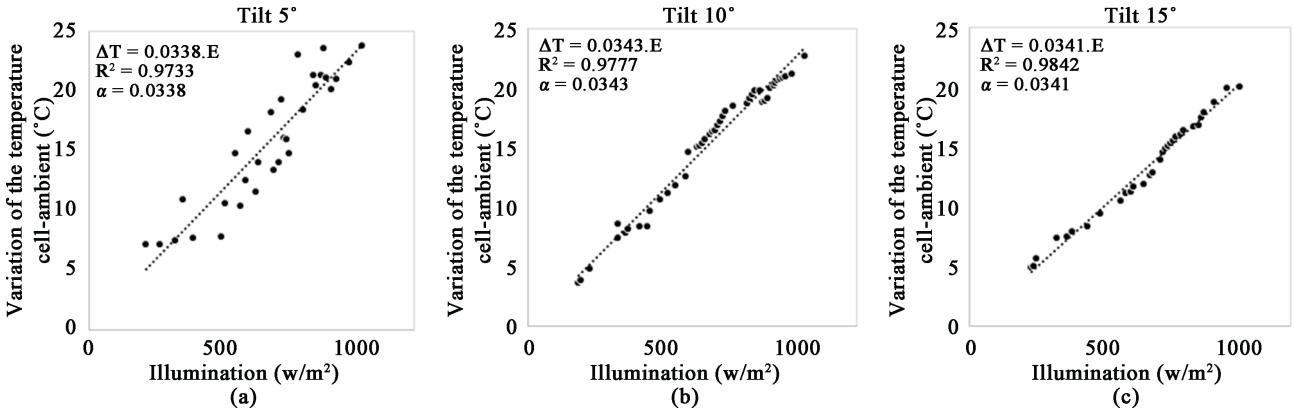

Figure 14. Variation of the temperature difference between cell and ambient air according to the illumination.

The difference ΔT between cell (T_c) and ambient (T_a) temperatures is in the form:

$$\Delta T = \alpha \cdot E \tag{19}$$

From the value of α ($^\circ C \cdot m^2 \cdot w^{-1}$) determined experimentally in Figure 14, the nominal operating temperature of cell is deduced using relationship (20).

$$NOCT = 800\alpha + 20 \tag{20}$$

The ideality factor n of the diode is determined from the relation (3) which

can be in the form:

$$V_{co} = a \cdot \ln\left(I_{sc}\right) + b \tag{21}$$

From the value of the coefficients a (V/A) and b (V) determined experimentally in Figure 15, the value of this factor n is determined to the relation (22).

$$n = \frac{q \cdot a}{KT} \tag{22}$$

The values of the cell utilization limit temperature (NOCT) and the diode ideality factor (n) are summarized in Table 6. The experimental constants a and a were determined at the temperature of 45˚C.

Under site conditions, the nominal operating cell temperature is 47˚C and the diode ideality factor is between 1.5 and 2.

3.4. Efficiency of the Photovoltaic Module in the Conditions of the Site

The form factor (FF) of the cell and the maximum efficiency (η) allow to evaluate the performance of the module in the conditions of the site. The values of FF and η are respectively determined using relations (23) and (24).

$$\mathrm{FF} = \frac{V_m \cdot I_m}{V_{oc} \cdot I_{sc}} = \frac{P_m}{V_{oc} \cdot I_{sc}} \tag{23}$$

$$\eta = \frac{P_m}{E \cdot S} \tag{24}$$

In relation (24), S, equal to 1.246 m^2, is the useful area of the photovoltaic

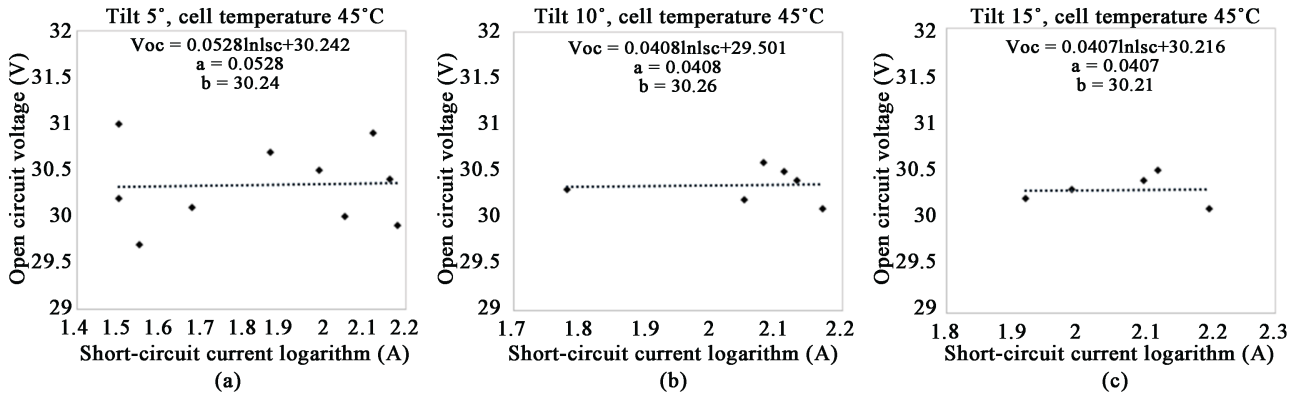

Figure 15. Graphic determination of the ideality factor of the diode.

Table 6. Values of the nominal operating cell temperature and the diode ideality factor.

Tilt angle	(˚C·m²/w)	*a* (V/A)	NOCT (˚C)	*n*
5˚	0.0338	0.0528	47.0	1.9
10˚	0.0343	0.0408	47.4	1.5
15˚	0.0341	0.0407	47.3	1.5

module. Table 7 summarizes the maximum values of the cell form factor and the conversion efficiency of the PV module under site conditions.

The maximum form factor obtained in the site conditions is 67%. The performance of the solar cell leads to a maximum conversion efficiency of the onsite module equal to 15%. Under STC conditions, the photovoltaic module is likely to produce a maximum return of 23% with a cell form factor of 75%. These results show clearly the influence of the meteorological factors of the implantation site on the performance parameters of the photovoltaic panel. The curves of evolution of the form factor and the conversion efficiency are presented respectively in Figure 16 and Figure 17.

For the three tilts, the form factor FF increases linearly with a small slope as a function of illumination. All values are between 50% and 70%. For a given illumination value, the form factor increases slightly for cell temperatures between 35˚C and 47˚C. Beyond 47˚C, a slight degradation of the performance of the solar cell is noted. The heating of the photovoltaic cell reduces its efficiency.

For the three inclinations, the highest values of the efficiency are obtained with the 10˚ configuration of the solar collector. The shape of the curves in the Figure 17 shows that the overall efficiency decreases from 15% to 12% when the

Table 7. Maximum values of form factor and module conversion efficiency.

Parameters	Tilt angle		
	5˚	10˚	15˚
E (w/m²)	1009	1009	1009
I_{sc} (A)	9.6	9.3	9.3
V_{oc} (V)	30.5	30.4	30.4
P_m (w)	177.6	190.1	172
FF	60.7	67.2	60.8
η	14.1	15.1	13.7

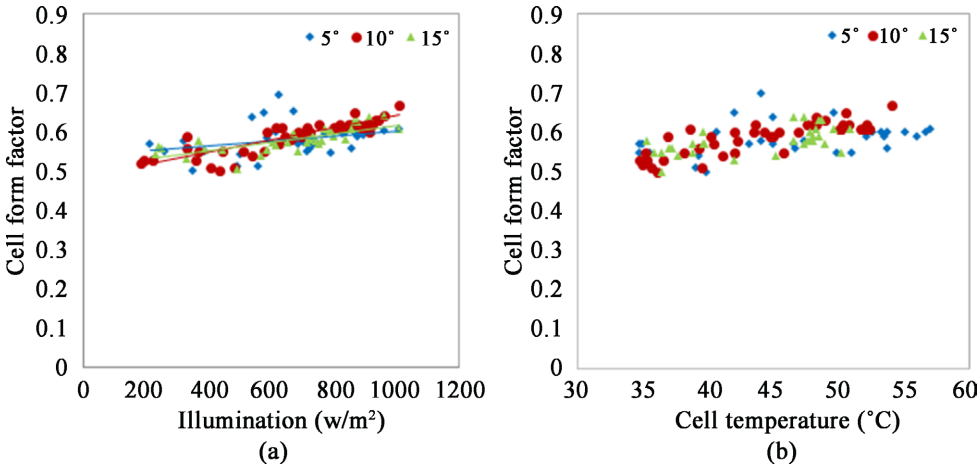

Figure 16. Evolution of the cell form factor according to the illumination and the temperature.

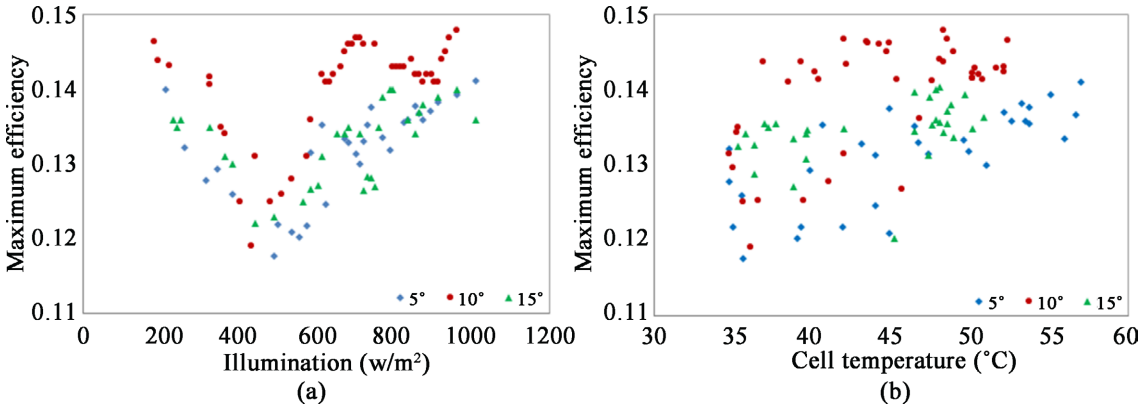

Figure 17. Evolution of the maximum conversion efficiency of the module according to the illumination and the temperature.

illumination increases between 200 and 500 w/m². On the other hand, from 500 w/m² to about 800 w/m², the efficiency increases with illumination. For the 10˚ tilt of the PV module, the efficiency decreases again from 15% to 14% between 800 w/m² and 1000 w/m². This decrement in efficiency for illuminations greater than 800 w/m² is due to the degradation of the cell's performance beyond its operating temperature limit (47˚C).

The performance of the photovoltaic panel is significantly improved for a tilt angle of 10˚. In the meteorological conditions of the site, the 10˚ angular configuration is the best profile of the three tilts chosen for any photovoltaic installation.

4. Conclusions

This characterization of the monocrystalline photovoltaic module of 250 wp, although it is not easy to evaluate the characteristics of performance of this one in real situation according to the meteorological conditions that imposed the site of implantation. The analysis of the stability of these parameters in the face of the most important external factors, namely the illumination, the temperature, and the tilt angle, helps us to define the extreme modalities of operation of a photovoltaic module according to the weather conditions of the site. In practice, the electrical characteristics of the module have been evaluated which led to an overall conversion efficiency of 15% for a maximum power that could be delivered at maximum illumination (1009 w/m²) of the order of 190 w. The results showed the strong dependence of these internal characteristics of the module with the illumination and the cell's temperature. A degradation of the energy performances of the cell has been recorded which was accentuated beyond 47˚C (NOCT). The voltage and power degradation coefficients were estimated respectively at −0.0864 V/˚C and −1.6248 w/˚C. On the other hand, the judicious choice of the tilt angle of the PV module makes it possible to improve the performances of this one. Thus, for this study, the 10˚ position proved to be ideal for optimizing the overall efficiency of the photovoltaic pane.

Finally, the solar panel studied has good overall performance and that it can be used appropriately for the mission that will be assigned to it.

Acknowledgments

The authors thank the Strategic Support Program for Scientific Research of Côte d'Ivoire (PASRES) for their support in the acquisition of the material used to do the study.

Conflicts of Interest

The authors declare no conflicts of interest regarding the publication of this paper.

References

[1] Mathieu, A. (2012) Contribution à la conception et à l'optimisation thermodynamique d'une microcentrale solaire thermoélectrique. Thèse de Doctorat (Sciences), Université de Lorraine, Lorraine.

[2] Howland, M.F., *et al.* (2022) Collective Wind Farm Operation Based on a Predictive Model Increases Utility-Scale Energy Production. *Nature Energy*, **7**, 818-827. https://doi.org/10.1038/s41560-022-01085-8

[3] Armaroli, N. and Balzani, V. (2016) Solar Electricity and Solar Fuels: Status and Perspectives in the Context of the Energy Transition. *Chemistry—A European Journal*, **22**, 32-57. https://doi.org/10.1002/chem.201503580

[4] Sivaram, V. (2018) Taming the Sun: Innovations to Harness Solar Energy and Power the Planet. MIT Press, Cambridge. https://doi.org/10.7551/mitpress/11432.001.0001

[5] Seibert, M.K. and Rees, W.E. (2021) Through the Eye of a Needle: An Eco-Heterodox Perspective on the Renewable Energy Transition. *Energies*, **14**, Article No. 4508. https://doi.org/10.3390/en14154508

[6] Unuofin, J.O., Iwarere, S.A. and Daramola, M.O. (2023) Embracing the Future of Circular Bio-Enabled Economy: Unveiling the Prospects of Microbial Fuel Cells in Achieving True Sustainable Energy. *Environmental Science and Pollution Research*, **30**, 90547-90573. https://doi.org/10.1007/s11356-023-28717-0

[7] Shah, H.H., Bareschino, P., Mancusi, E. and Pepe, F. (2023) Environmental Life Cycle Analysis and Energy Payback Period Evaluation of Solar PV Systems: The Case of Pakistan. *Energies*, **16**, Article No. 6400. https://doi.org/10.3390/en16176400

[8] Seri, M., Mercuri, F., Ruani, G., Feng, Y., Li, M., Xu, Z.X. and Muccini, M. (2021) Toward Real Setting Applications of Organic and Perovskite Solar Cells: A Comparative Review. *Energy Technology*, **9**, Article ID: 2000901. https://doi.org/10.1002/ente.202000901

[9] Kassmi, K., Hamdoui, M. and OliviÉ, F. (2007) Conception et modélisation d'un système photovoltaïque adapté par une commande mppt analogique. *Revue Des Energies Renouvelables*, **10**, 451-462. https://doi.org/10.54966/jreen.v10i4.749

[10] Yan, J. and Saunders, B.R. (2014) Third-Generation Solar Cells: A Review and Comparison of Polymer: Fullerene, Hybrid Polymer and Perovskite Solar Cells. *RSC Advances*, **4**, 43286-43314. https://doi.org/10.1039/C4RA07064J

[11] Müller-Buschbaum, P., Thelakkat, M., Fässler, T.F. and Stutzmann, M. (2017) Hybrid Photovoltaics—From Fundamentals towards Application. *Advanced Energy Materials*, **7**, Article ID: 1700248. https://doi.org/10.1002/aenm.201700248

[12] Venkateswararao, A. and Wong, K.T. (2021) Small Molecules for Vacuum-Processed

Organic Photovoltaics: Past, Current Status, and Prospect. *Bulletin of the Chemical Society of Japan*, **94**, 812-838. https://doi.org/10.1246/bcsj.20200330

[13] Luo, W., *et al.* (2017) Potential-Induced Degradation in Photovoltaic Modules: A Critical Review. *Energy & Environmental Science*, **10**, 43-68. https://doi.org/10.1039/C6EE02271E

[14] Karduri, R.K.R. and Ananth, C. (2023) Advancements in Photovoltaic Materials for Sustainable Energy Generation. *International Journal of Advanced Research in Basic Engineering Sciences and Technology* (*IJARBEST*). https://doi.org/10.2139/ssrn.4637813

[15] Fassinou, W.F. (1997) Réfrigérateur solaire photovoltaïque à trois compartiments avec batterie de froid: Etude, réalisation et analyse des irréversibilités. Thèse de Doctorat 3eme Cycle en Sciences, Université Nationale de Côte D'ivoire, Abidjan.

[16] Brou, T. (2010) Etude technico-économique des technologies solaires en Côte D'ivoire. Mémoire de Master, Institut International D'ingénierie de L'eau et de L'environnement (2ie), Burkina Faso.

[17] Kouassi, A.P.A., Touré, S. and Traoré, D. (2020) Seasonal Variability of the Solar Energy Potential of the City of Abidjan: Experimental Comparative Study of Two Sunshine Measurement Techniques. *Journal of Solar Energy Engineering*, **14**, Article ID: 011013. https://doi.org/10.1115/1.4044566

[18] Markvart, T. and Castaner, L. (2003) Practical Handbook of Photovoltaics: Fundamentals and Applications. Elsevier, Amsterdam, 998.

[19] Khezzar, R., Zereg, M. and Khezzar, A. (2010) Comparaison entre les différents modèles électriques et détermination des paramètres de la caractéristique i-v d'un module photovoltaïque. *Revue des Energies Renouvelables*, **13**, 379. https://doi.org/10.54966/jreen.v13i3.206

[20] Ricaud, A. (2013) Les politiques publiques de l'énergie solaire. *Annales Historiques de L' electricité*, *Editions Victoires*, **1**, 111-131. https://doi.org/10.3917/ahe.011.0111

[21] Bashahu, M. and Habyarimana, A. (1995) Review and Test of Method for Determination of the Solar Cell Series Resistance. *Renewable Energy*, **6**, 129-138. https://doi.org/10.1016/0960-1481(94)E0021-V

[22] Priyanka, S., Lal, M. and Singh, S.N. (2007) A New Method of Determination of Series and Shunt Resistances of Silicon. *Solar Energy Materials and Solar Cells*, **91**, 137-142. https://doi.org/10.1016/j.solmat.2006.07.008

[23] Bouazidi, K., Chegaard, M. and Bouhemadou, A. (2007) Solar Cells Parameters Evaluation Considering the Series and Shunt Resistance. *Solar Energy Materials and Solar Cells*, **18**, 1647-1651. https://doi.org/10.1016/j.solmat.2007.05.019

[24] Khezzar, R., Zereg, M. and Khezzar, A. (2010) Comparaison entre les différents modèles électriques et détermination des paramètres de la caractéristique i-v d'un module photovoltaïque. *Revue des Energies Renouvelables*, **13**, 379-388. https://doi.org/10.54966/jreen.v13i3.206

[25] Agarwal, S.K., Muralidharan, R., Jain, S.C., Agarwala, A. and Tewary, V.K. (1981) A New Method for Measurement of Series Resistance of Solar Cell. *Journal of Physics D*: *Applied Physics*, **14**, 1643-1646. https://doi.org/10.1088/0022-3727/14/9/011

[26] Wang, J.C., *et al.* (2011) A Novel Method for the Determination of Dynamic Resistance for Photovoltaic. *Energy*, **36**, 5968-5974. https://doi.org/10.1016/j.energy.2011.08.019

[27] Brigand, S. (2008) Les principes de l'énergie solaire photovoltaïque. Techniques De Construction, Editions Le Moniteur, Paris, 17.

Nomenclature

I: Module current
V: Module voltage
I-V: Current-voltage characteristic
P-V: Power-voltage characteristic
I_{ph}: Photocurrent
I_{sc}: Short-circuit current
V_{oc}: Open circuit voltage
I_m: Maximum useful current
V_m: Maximum useful voltage
P_m: Maximum useful power
E: Instantaneous illumination
PV: Photovoltaic
I_s: Saturation current of the diode
R_s: Series resistance
R_{sh}: Shunt resistance
R_c: Resistance of the platinum probe
ΔI: Variation between short-circuit current and maximum useful current
T: Temperature
T_a: Ambient temperature
T_c: Cell temperature
NOCT: Nominal operating cell temperature
n: Ideality factor of the diode
K: Boltzann constant
q: Elementary charge